

Quasiparticle energies for large molecules: a tight-binding GW approach

T.A. Niehaus,¹ M. Rohlfing,² F. Della Sala,³ A. Di Carlo,⁴ and Th. Frauenheim¹

¹ *Dept. of Theoretical Physics, University of Paderborn, D - 33098 Paderborn, Germany*

² *International university of Bremen, School of Engin. & Science, P.O. Box 750561, D-28725 Bremen, Germany*

³ *National Nanotechnology Laboratories of INFN, Università di Lecce,*

Distretto Tecnologico, Via Arnesano, 73100 Lecce, Italy

⁴ *INFN and Dept. of Electronic Engineering, University of Rome "Tor Vergata", 00133 Rome, Italy*

(Dated: September 1, 2021)

We present a tight-binding based GW approach for the calculation of quasiparticle energy levels in confined systems such as molecules. Key quantities in the GW formalism like the microscopic dielectric function or the screened Coulomb interaction are expressed in a minimal basis of spherically averaged atomic orbitals. All necessary integrals are either precalculated or approximated without resorting to empirical data. The method is validated against first principles results for benzene and anthracene, where good agreement is found for levels close to the frontier orbitals. Further, the size dependence of the quasiparticle gap is studied for conformers of the polyacenes ($C_{4n+2}H_{2n+4}$) up to $n = 30$.

I. INTRODUCTION

Density functional theory (DFT) has nowadays become the standard tool for the description of ground state properties of such different systems as atoms, molecules, clusters or bulk materials. Part of the success stems from the fact that in the DFT electron correlation is in principle exactly covered at the level of an effective one-particle Hamiltonian. Difficulties arise however, when the orbital energies obtained from the solution of the Kohn-Sham (KS) eigenvalue problem are interpreted as approximate quasiparticle energies, i.e., the energies associated with addition or removal of an electron. A well known example is the severe underestimation of the band gap in insulating solids or semiconductor crystals [1]. The same problem is also present in molecules. Although it has been shown that Koopmans theorem also holds for the highest occupied molecular orbital (HOMO) in DFT [2], ionization potentials come out too small in practical calculations. This fact has been traced back to the wrong asymptotic behavior of common approximate exchange-correlation (XC) functionals like the local density approximation (LDA) [3]. However, the KS gap can be shown to represent a first-order approximation to optical excitation energies [4], and thus the KS gap will be different from the quasiparticle gap even if the exact XC functional is used.

As an alternative to DFT, many body perturbation theory in the approximation of Hedin [5] has been extremely successful in the prediction of quasiparticle spectra. In this so-called GW method the description of the electron-electron interaction is approached in a different way than in DFT. While the exchange energy is exactly calculated like in Hartree-Fock theory, correlation is accounted for by an energy dependent dielectric function which reduces the coulomb interaction between electrons. The scheme is nearly self-interaction free and provides asymptotically correct potentials. Consequently, the band gap problem of the DFT is absent in the GW and also ionization potentials and electron affinities of

molecules are computed in good accord with experiment [6, 7, 8, 9].

In conjunction with the solution of the Bethe-Salpeter (BS) equation [10, 11, 12], the GW approximation can also be used to calculate charge neutral quasiparticle excitations, i.e., optical spectra. In this context, the time-dependent generalization of DFT [13], which in principle provides the same information as GW+BS has in practice been found to give inferior results for the absorption spectrum of solids [14]. Also for molecules, time dependent DFT fails in the description of charge transfer excitations [15], which was attributed to the locality of common XC-functionals [16, 17, 18]. Again, GW+BS which contains the correct long range electron-hole interaction should be able to remedy the problem.

Another example where DFT orbital energies are widely used but lead to problematic results is given by transport calculations in molecular devices. Here the calculated currents differ typically by orders of magnitudes from the experimentally found values [19, 20, 21]. Since the current-voltage characteristics of such systems depend critically on the HOMO-LUMO gap, a major improvement is expected when GW quasiparticle energies would be used instead of DFT orbital energies.

It is clear from the forgoing discussion, that although the GW approximation was developed in the context of solid state theory, its application to molecular systems is becoming more and more important. In fact, implementations for systems with translational symmetry using plane wave basis sets can directly be applied to finite systems when very large super-cells are used. Nonetheless, the use of localized atomic-like basis sets is clearly more adapted to the problem and such implementations have been utilized quite successful in the past years [6, 7, 22, 23]. But even with this improvement, the numerical complexity of the GW equations limits a first principles evaluation to rather small system sizes of tens of atoms. So applications like transport calculations for molecules, where a sizable amount of the atoms comprising the leads need to be included, or molecular dy-

namics in the excited state are currently not feasible. It would therefore be desirable to have an approximate GW scheme which nevertheless captures the essential physics of the underlying theory. The purpose of this paper is to propose such a scheme.

In the past years a number of different approximated GW methods have been introduced and successfully applied [5, 24, 25, 26, 27, 28, 29, 30, 31, 32]. The main difference to this earlier work is that we focus on molecular applications with a real space implementation. Furthermore we try to avoid empirical parameters in order to achieve a higher transferability.

Like GW calculations usually employ DFT energies and wavefunctions as zero order approximations to the quasiparticle quantities, our approach is based on the *Density Functional based Tight-Binding* (DFTB) method [33, 34], which itself is an approximation to DFT. The DFTB scheme has been shown to provide reliable results on a variety of systems classes ranging from molecules to solids at a highly reduced numerical cost compared to DFT calculations. In section II the DFTB method is briefly introduced together with a detailed description of the approximations in the various quantities involved in the GW formalism. The accuracy and main shortcomings of our approach are then examined in section III, where it is applied to a prototype series of π -bonding molecules, the polyacenes.

II. METHODOLOGY

The GW method has been extensively discussed in the literature and several reviews are available [14, 36, 37, 38, 39]. The main goal is to solve the Dyson equation:

$$\left(H_0 + \Sigma(\epsilon_i^{QP})\right) |\psi_i^{QP}\rangle = \epsilon_i^{QP} |\psi_i^{QP}\rangle, \quad (1)$$

for the quasiparticle energies ϵ_i^{QP} and wavefunctions $|\psi_i^{QP}\rangle$. Here H_0 is the Hartree Hamiltonian and the so-called self-energy Σ is a nonlocal and energy dependent operator, which accounts for exchange and correlation effects. It thus can be seen as a replacement for the local exchange-correlation potential v_{xc} in the DFT Kohn-Sham (KS) equations. In the GW approximation of Hedin, the self-energy is given as a product of the single-particle Greens function G and the screened Coulomb interaction W . As these quantities, as well as the Hartree Hamiltonian, depend on the quasiparticle wavefunctions, the Dyson equation [Eq. (1)] has to be iterated until self-consistency is achieved. However, since the DFT one-particle wavefunctions are usually very similar to the final quasiparticle ones and moreover self-consistency not necessarily improves the result [40], Eq. (1) may be simplified to

$$\epsilon_i^{QP} = \epsilon_i^{DFT} + Z_i \langle \psi_i | \Sigma(\epsilon_i^{DFT}) - v_{xc} | \psi_i \rangle, \quad (2)$$

where ψ_i are KS orbitals, non-diagonal elements of the Dyson Hamiltonian in the basis of DFT states are ne-

glected and the energy dependence of the self-energy has partially been accounted for by the renormalization constant Z_i :

$$Z_i = \left(1 - \frac{\partial \Sigma(\omega)}{\partial \omega} \Big|_{\epsilon_i^{DFT}}\right)^{-1}. \quad (3)$$

In our approach Eq. (2) is now subjected to further approximations which are presented separately for each term in the following.

A. The DFT orbital energies ϵ_i^{DFT}

As already mentioned, the Kohn-Sham energies ϵ_i^{DFT} and orbitals are obtained from the DFTB method, which has been presented in detail earlier (for a review see Ref. [41]). Here we only describe the method to the extent necessary to motivate the remaining approximations in this work. In the DFTB, the Kohn-Sham states ψ_i^{DFTB} are expanded in a linear combination of atom centered orbitals ϕ_μ :

$$\psi_i(\mathbf{r}) = \sum_{\mu} c_{\mu i} \phi_{\mu}(\mathbf{r} - \mathbf{R}_A), \quad (4)$$

which are obtained from a preceding DFT calculation on neutral atoms. Here $\mu := \{Alm\}$ is a compound index indicating the atom on which the basisfunction is centered, its angular momentum l and magnetic quantum number m . Later, also quantities which depend only on A and l appear. These will be denoted with a corresponding index $\bar{\mu} := \{Al\}$ throughout the paper.

Since atomic orbitals are usually too long ranged to be used directly in a molecular calculation, the atomic DFT Hamiltonian is augmented with a confining square potential to compress the wavefunction outside of a given radius r_0 (usually twice the covalent radius of the element), while ensuring the desired cusp conditions inside [33]. From the atomic valence states a minimal basis of s and p orbitals is then chosen, although also d -orbitals are included when necessary, e.g. for second row elements [42]. With the help of the expansion (4) the Kohn-Sham equations of DFT can be written:

$$\sum_{\nu} c_{\nu i} (H_{\mu\nu} - \epsilon_i S_{\mu\nu}) = 0, \quad \forall \mu, i \quad (5a)$$

$$S_{\mu\nu} = \langle \phi_{\mu} | \phi_{\nu} \rangle \quad (5b)$$

$$H_{\mu\nu} = H_{\mu\nu}^0 + H_{\mu\nu}^{SCC}, \quad (5c)$$

where the overlap matrix $S_{\mu\nu}$ has been introduced and the Hamiltonian is divided in two parts. The first part $H_{\mu\nu}^0$ is approximated as follows:

$$H_{\mu\nu}^0 = \begin{cases} \epsilon_{\mu}^{\text{free atom}} & : \mu = \nu \\ \langle \phi_{\mu}(\mathbf{r}) | H_{DFT} [\rho_A^0 + \rho_B^0] | \phi_{\nu}(\mathbf{r}) \rangle & : \mu \in A, \nu \in B \\ 0 & : \text{otherwise} \end{cases} \quad (6)$$

The KS Hamiltonian in Eq. (6) contains as usual the kinetic energy, the electron-nuclei attraction and the Hartree as well as exchange-correlation potential and depends only on the atomic densities of atoms A and B . This means, that besides the crystal field terms also all three-center terms are neglected. The onsite elements are given as atomic orbital energies obtained from a DFT calculation without confining potential to ensure the right dissociation limit. The integrals in Eq. (6) are numerically evaluated and tabulated for varying distance between atoms A and B .

The second part of the Hamiltonian (5c) corrects for the fact that the molecular density differs from a simple superposition of atomic densities. In order to estimate this difference, spherical averages over basis functions belonging to one angular momentum shell are build

$$F_{Al}(\mathbf{r}) = \frac{1}{2l+1} \sum_{m=-l}^{m=l} |\phi_{Alm}(\mathbf{r})|^2, \quad (7)$$

and used in a Mulliken type approximation

$$\phi_{\mu}(\mathbf{r})\phi_{\nu}(\mathbf{r}) \approx \frac{1}{2} S_{\mu\nu} (F_{\bar{\mu}}(\mathbf{r}) + F_{\bar{\nu}}(\mathbf{r})), \quad (8)$$

to represent the molecular density. The latter is then constructed from point charges

$$\begin{aligned} \rho(\mathbf{r}) &= \sum_i |\psi_i(\mathbf{r})|^2 \approx \sum_{\bar{\mu}} q_{\bar{\mu}} F_{\bar{\mu}}(\mathbf{r}) \\ \text{with } q_{\bar{\mu}} &= \sum_{m=-l}^l \sum_{\nu i} c_{\mu i} c_{\nu i} S_{\mu\nu}; \end{aligned} \quad (9)$$

an expansion, which despite of its simplicity takes the different spatial localization of e.g s and p -orbitals into account. Based on these considerations, the difference between the true molecular density and superimposed atomic densities can be estimated with net Mulliken charges $\Delta q_{\bar{\mu}} = q_{\bar{\mu}} - q_{\bar{\mu}}^{\text{atom}}$ and leads to the correction term [35]:

$$H_{\mu\nu}^{SCC} = \frac{1}{2} S_{\mu\nu} \sum_{\bar{\delta}} (\gamma_{\bar{\mu}\bar{\delta}} + \gamma_{\bar{\nu}\bar{\delta}}) \Delta q_{\bar{\delta}}, \quad (10)$$

as shown in more detail in Ref. [34].

The term γ describes the interaction of two electrons in the orbitals $\bar{\mu}$ on atom A and $\bar{\nu}$ on atom B , including the effects of exchange and correlation:

$$\gamma_{\bar{\mu}\bar{\nu}} = \iint F_{\bar{\mu}}(\mathbf{r}) \left(\frac{1}{|\mathbf{r} - \mathbf{r}'|} + \frac{\delta v_{xc}[\rho(\mathbf{r})]}{\delta \rho(\mathbf{r}')} \right) F_{\bar{\nu}}(\mathbf{r}') d\mathbf{r} d\mathbf{r}' \quad (11a)$$

$$\approx \gamma_{\bar{\mu}\bar{\nu}}(|\mathbf{R}_A - \mathbf{R}_B|, U_{\bar{\mu}}^H, U_{\bar{\nu}}^H), \quad (11b)$$

and is approximated by considering two limiting cases. For large distances between the two atoms, the integral (11a) simplifies to a pure Coulomb interaction of two

point charges, since the v_{xc} contribution dies off rapidly. For short distance on the other hand, Eq. (11a) becomes an atomic integral U_H , which can be easily calculated numerically for each element. From these limiting cases a simple interpolation formula was derived in Ref. [34], which is a function of the atomic parameters U^H and the interatomic distance only. Since the Mulliken net charges $\Delta q_{\bar{\delta}}$ depend on the molecular orbital coefficients $c_{\mu i}$, Eq. (5a) has to be iterated until self-consistency. As a result the orbital energies ϵ_i^{DFTB} needed in Eq. (2) are obtained.

B. The self-energy $\Sigma_i(\epsilon)$

We calculate the self-energy in the GW approximation by:

$$\Sigma(\mathbf{r}, \mathbf{r}', \epsilon) = \frac{i}{2\pi} \int e^{i\omega 0^+} G_0(\mathbf{r}, \mathbf{r}', \epsilon - \omega) W(\mathbf{r}, \mathbf{r}', \omega) d\omega, \quad (12)$$

where G_0 is the single particle Greens function built from DFTB wavefunctions and $W = \epsilon^{-1}v$ is the screened Coulomb interaction, while v is the bare one. For the following it is beneficial to divide the self-energy into two parts as $\Sigma = iG_0v + iG_0(\epsilon^{-1} - 1)v$. The latter term denoted Σ^c is energy dependent and describes dynamical correlation effects, while the former term Σ^x provides the major part of the self-energy. For Σ^x the frequency integration in Eq. (12) can be carried out easily and yields in the KS basis the usual Hartree-Fock exchange energy for orbital i :

$$\Sigma_i^x = \sum_j^{\text{occ}} \iint \frac{\psi_i(\mathbf{r})\psi_j(\mathbf{r})\psi_i(\mathbf{r}')\psi_j(\mathbf{r}')}{|\mathbf{r} - \mathbf{r}'|} d\mathbf{r} d\mathbf{r}'. \quad (13)$$

Since in contrast to empirical tight-binding schemes the basis functions ϕ_{μ} are available in the DFTB method, one could in principle calculate Eq. (13) directly from the wavefunctions. In this way the method would scale like first principles schemes with N^4 , where N is the number of basis functions. Therefore we seek for an approximate solution and note that after expansion of the KS states in atomic orbitals, Eq. (13) contains products of basis functions which are in general located on different atomic centers. An important simplification can thus be achieved, when the Mulliken approximation [Eq. (8)] is applied to the integral. Introducing the following notation for the matrix elements of a general two-point function in the basis of squared and spherically averaged DFTB atomic orbitals:

$$[f]_{\bar{\mu}\bar{\nu}} = \iint F_{\bar{\mu}}(\mathbf{r}) f(\mathbf{r}, \mathbf{r}') F_{\bar{\nu}}(\mathbf{r}') d\mathbf{r} d\mathbf{r}', \quad (14)$$

we then arrive at the following simplified expression for Σ_i^x :

$$\Sigma_i^x = \sum_j^{\text{occ}} \sum_{\bar{\mu}\bar{\nu}} q_{\bar{\mu}}^{ij} [v]_{\bar{\mu}\bar{\nu}} q_{\bar{\nu}}^{ij}. \quad (15)$$

Here the q_{μ}^{ij} are generalized Mulliken charges

$$q_{\mu}^{ij} = \frac{1}{2} \sum_{m=-l}^l \sum_{\nu} (c_{\mu i} c_{\nu j} S_{\mu\nu} + c_{\nu i} c_{\mu j} S_{\nu\mu}), \quad (16)$$

which provide a point charge representation of the overlap between two molecular orbitals i and j . The important observation is now that the matrix of the Coulomb interaction is equal to the definition of the γ -functional in Eq. (11a), when the contributions stemming from the XC functional are removed. In other words, the functional form of γ can also be used for $[v]$, if the atomic parameters U^H are replaced by the parameters U^{ee} which incorporate only the classical Coulomb interaction. We calculate these electron repulsion integrals directly from the DFTB basis functions using the algorithms presented in Ref. [43]. The parameters for each angular momentum are set to an average over the integrals for different combinations of the magnetic quantum numbers belonging to that shell.

The main drawback of the Mulliken approximation in Eq. (8) is, that onsite integrals of the exchange type are completely neglected. These, however, contribute around 10 % to the final exchange energy. Similar to the proceeding in the quantum chemical INDO approach [44] we therefore include all non-vanishing onsite integrals, leading to the following final form for Σ_i^x [45]:

$$\begin{aligned} \Sigma_i^x &= \sum_j^{occ} \sum_{\bar{\mu}\bar{\nu}} q_{\mu}^{ij} [v]_{\bar{\mu}\bar{\nu}} q_{\nu}^{ij} \\ &+ \sum_A \sum_{\mu, \nu \ni A}^{\mu \neq \nu} (c_{\mu i}^2 c_{\nu j}^2 + c_{\mu i} c_{\nu j} c_{\nu i} c_{\mu j}) (\phi_{\mu} \phi_{\nu} | \phi_{\mu} \phi_{\nu}). \end{aligned} \quad (17)$$

While in the INDO approach the necessary integrals are taken as empirical fitting parameters, we compute them from the atomic basis functions. More precisely, the parameters are calculated from an uncompressed wavefunction in order to be consistent with the onsite definition of the DFTB Hamiltonian matrix elements. The values used in this study are given in Tab. I together with the U^H and U^{ee} parameters.

Let us now turn to the correlation contribution of the self-energy Σ^c , which is much harder to evaluate, since it amounts to a multi step procedure. First we construct matrix elements of the electronic polarizability in the random-phase approximation according to:

$$\begin{aligned} [P(\omega)]_{\bar{\mu}\bar{\nu}} &= 2 \sum_k^{occ} \sum_l^{virt} \left(\sum_{\bar{\alpha}} \tilde{S}_{\bar{\mu}\bar{\alpha}} q_{\bar{\alpha}}^{kl} \right) \left(\sum_{\bar{\beta}} q_{\bar{\beta}}^{kl} \tilde{S}_{\bar{\beta}\bar{\nu}} \right) \times \\ &\left[\frac{1}{\epsilon_k^{DFTB} - \epsilon_l^{DFTB} - \omega + i0^+} + \frac{1}{\epsilon_k^{DFTB} - \epsilon_l^{DFTB} + \omega + i0^+} \right], \end{aligned} \quad (18)$$

where we again used the Mulliken approximation of Eq. (8) and introduced the overlap matrix of spherically

TABLE I: The atomic electron-electron interaction integrals U_l^H and U_l^{ee} , as well as the exchange integrals $(\phi_{lm}\phi_{l'm'}|\phi_{lm}\phi_{l'm'})$ used in this study. Results are given for free and compressed atomic basisfunctions, as defined by the confinement radius r_0 (see Sec. II A and Ref. [33]). The same compression is used in the calculation of the Hamiltonian and overlap matrix elements.

Element	Parameter	r_0 [a.u.]	Value [eV]
Hydrogen	U_0^H	∞	11.06
	U_0^{ee}	∞	15.39
	U_0^{ee}	3.0	21.36
Carbon	U_0^H	∞	10.81
	U_1^H	∞	10.81
	U_0^{ee}	∞	15.66
	U_1^{ee}	∞	14.15
	U_0^{ee}	2.7	17.98
	U_1^{ee}	2.7	18.72
	$(\phi_{00}\phi_{1m'} \phi_{00}\phi_{1m'})$	∞	3.01
	$(\phi_{1m}\phi_{1m'} \phi_{1m}\phi_{1m'})$	∞	0.75

averaged DFTB basis functions $\tilde{S}_{\bar{\mu}\bar{\nu}} = \int F_{\bar{\mu}}(\mathbf{r}) F_{\bar{\nu}}(\mathbf{r}) d\mathbf{r}$, not to be confused with the overlap appearing in the KS equations (5b).

The quantity \tilde{S} never needs to be constructed, since it appears only in intermediate quantities and falls out in the final equation for the screened Coulomb interaction we are aiming at.

In a next step we obtain the dielectric function in matrix notation as:

$$[\epsilon(\omega)] = \tilde{S} - [v] \tilde{S}^{-1} [P(\omega)]. \quad (19)$$

For systems with translational symmetry the dielectric matrix is hermitian in reciprocal space. This fact is used in plasmon-pole models [24, 46, 47] to simplify the frequency integration in Eq. (12), which is numerically demanding due to the complicated pole structure of ϵ^{-1} along the real axis. In these models the inverse of the dielectric matrix is diagonalized and the eigenvalues are assumed to be a simple function of the frequency, while the eigenvectors are frequency independent. Free parameters of the model are either obtained from sum rules or by diagonalizing ϵ^{-1} at different test frequencies. It is then easy to perform the frequency integration analytically to obtain the self-energy.

However, in the present real-space approach the inverse dielectric matrix is not symmetric. In Ref. [22] this problem was circumvented by introducing an auxiliary symmetrized dielectric matrix, while we proceed by noting that the screened Coulomb interaction W :

$$[W(\omega)] = \tilde{S} [\epsilon(\omega)]^{-1} [v], \quad (20)$$

has the desired property of being symmetric. Applying the plasmon-pole approximation to $[W - v]$, we finally

arrive at the following expression for the correlation contribution to the self-energy for orbital i :

$$\Sigma_i^c(\omega) = \sum_n \sum_{\bar{\delta}} \left(\sum_{\bar{\mu}} q_{\bar{\mu}}^{in} \Phi_{\bar{\mu}\bar{\delta}} \right)^2 \times \frac{z_{\bar{\delta}} \omega_{\bar{\delta}}}{2} \begin{cases} \frac{1}{\omega - \epsilon_n^{\text{DFTB}} + \omega_{\bar{\delta}}} & : n \in \text{occ} \\ & : \\ \frac{1}{\omega - \epsilon_n^{\text{DFTB}} - \omega_{\bar{\delta}}} & : n \in \text{virt}, \end{cases} \quad (21)$$

where Φ denotes the eigenvectors of $[W - v]$, while $z_{\bar{\delta}}$ and $\omega_{\bar{\delta}}$ are the mentioned parameters of the plasmon-pole model, as defined in Ref. [22]. They are determined by diagonalization of $[W - v]$ at zero frequency and one frequency on the imaginary axis. We checked that the actual values chosen have little impact (< 0.1 eV) on the final quasiparticle energies.

Based on the self-energy, the renormalization constant Z_i from Eq. (2) is then obtained by a simple numerical differentiation. For the molecular structures we studied, Z_i is usually roughly 0.85, which is close to the values reported for bulk systems [24]. However, for certain unbound virtual orbitals, Z_i can decrease to as much as 0.5.

C. The exchange-correlation contribution v_i^{xc}

We complete the description of our method with an investigation of the contributions to the quasiparticle energies arising from the exchange-correlation potential, denoted $v_i^{xc}[\rho_v]$. As indicated, v_{xc} is evaluated at the valence density ρ_v , consistent with the fact that the summation in the exchange energy [Eq. (15)] is carried out over valence orbitals j only. As pointed out in Ref. [48], the core contribution to the exchange energy is not negligible and this holds also for the core contribution of v^{xc} . However, even for exchange-correlation potentials commonly used today, which are far from exact, both core contributions cancel to a large degree when computing quasiparticle energies according to Eq. (2).

In analogy to the derivation of the DFTB method, we now expand v^{xc} around the density ρ_v^0 , which is a superposition of atomic valence densities. With $\rho_v = \rho_v^0 + \delta\rho$ we obtain:

$$v_i^{xc}[\rho_v] = \int |\psi_i(\mathbf{r})|^2 v_i^{xc}[\rho_v^0(\mathbf{r})] d\mathbf{r} + \iint |\psi_i(\mathbf{r})|^2 \frac{\delta v_i^{xc}[\rho_v(\mathbf{r})]}{\delta \rho_v(\mathbf{r}')} \delta \rho(\mathbf{r}') d\mathbf{r} d\mathbf{r}' + \mathcal{O}(\delta \rho^2) \quad (22a)$$

$$\approx \sum_{\mu\nu} c_{\mu i} c_{\nu i} v_{\mu\nu}^{xc}[\rho_v^0] + \sum_{\bar{\mu}\bar{\nu}} q_{\bar{\mu}}^{ii} \left[\frac{\delta v^{xc}}{\delta \rho} \right]_{\bar{\mu}\bar{\nu}} \Delta q_{\bar{\nu}} \quad (22b)$$

In going from Eq. (22a) to Eq. (22b), the Mulliken approximation was again employed and matrix elements of the exchange-correlation kernel $\delta v^{xc}/\delta \rho$ were introduced in the notation of Eq. (14). The first term of Eq. (22b)

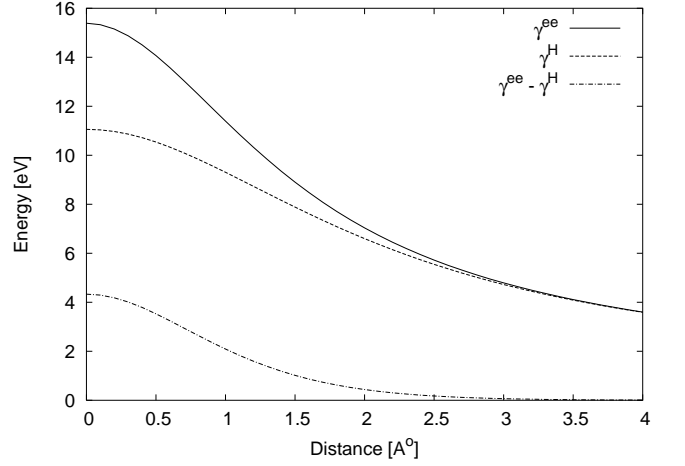


FIG. 1: The electron-electron interaction integrals for hydrogen as a function of distance. Shown are results including both Coulomb and exchange-correlation interactions (γ^H), pure Coulomb (γ^{ee}) and the *negative* of the pure exchange-correlation interaction ($-\delta v^{xc}/\delta \rho = \gamma^{ee} - \gamma^H$), according to Eq. (23).

is now exactly treated like the Hamiltonian in the DFTB scheme. That is, only the two-center terms are kept and the onsite values are calculated from uncompressed basis functions and atomic densities. Then the integrals are numerically evaluated and tabulated in the usual Slater-Koster form as a function of interatomic distance.

The second term in Eq. (22b) is the counterpart of $H_{\mu\nu}^{SCC}$ in Eq. (5c). If we set

$$\left[\frac{\delta v^{xc}}{\delta \rho} \right]_{\bar{\mu}\bar{\nu}} = \gamma_{\bar{\mu}\bar{\nu}}(|\mathbf{R}_A - \mathbf{R}_B|, U_{\bar{\mu}}^H, U_{\bar{\nu}}^H) - \gamma_{\bar{\mu}\bar{\nu}}(|\mathbf{R}_A - \mathbf{R}_B|, U_{\bar{\mu}}^{ee}, U_{\bar{\nu}}^{ee}), \quad (23)$$

the long range $1/R$ tail of the two γ -functions cancels (see Fig. 1), and one is left with a short ranged representation of the exchange-correlation kernel without introducing any new parameters or integral approximations. Moreover the v^{xc} contribution of the self-energy now cancels all related contributions in the orbital energies ϵ_i^{DFTB} as it should be [49].

At this point, all the necessary ingredients to calculate quasiparticle energies within the DFTB scheme have been presented. In the next section we analyze the strengths and weaknesses of the method by applying it to the polyacene series.

III. APPLICATIONS

A. Comparison to first principles results

The polyacenes ($C_{4n+2}H_{2n+4}$) are linear chains of anelated polycyclic aromatic hydrocarbons, as shown in Fig. 2. The monomer ($n = 1$) is benzene. Naphtalene is with

TABLE II: The different contributions to the quasiparticle (QP) energies and the QP energies themselves obtained from the method described in this work (DFTB) as well as from first principles calculations using Gaussian type orbitals (GTO). Shown are results for some levels close to the frontier orbitals of the benzene and anthracene molecules. All energies in eV.

		ϵ^i		v_{xc}^i		Σ_x^i		Σ_c^i		ϵ_{QP}^i	
State	Sym.	GTO	DFTB	GTO	DFTB	GTO	DFTB	GTO	DFTB	GTO	DFTB
Benzene											
A_{2u}	π	-9.37	-8.95	-12.82	-12.39	-17.15	-16.35	2.03	2.47	-11.67	-10.45
E_{2g}	σ	-8.34	-7.71	-15.05	-12.25	-19.49	-15.62	1.86	1.41	-10.92	-9.67
E_{1g}	π	-6.59	-6.64	-13.03	-12.30	-15.61	-14.98	0.59	0.87	-8.58	-8.46
E_{2u}	π^*	-1.30	-1.32	-12.64	-11.72	-7.58	-7.41	-1.74	-0.99	2.01	2.00
B_{2g}	π^*	0.92	2.29	-6.96	-11.19	-2.89	-6.33	-2.31	-2.84	2.67	4.31
Anthracene											
B_{3u}	π	-7.97	-7.62	-12.98	-12.25	-16.32	-15.61	1.98	2.27	-9.33	-8.71
B_{2g}	σ	-7.85	-7.28	-13.07	-12.17	-16.40	-15.32	2.01	1.90	-9.15	-8.53
A_u	π	-6.82	-6.78	-13.12	-12.24	-15.81	-15.11	1.38	1.66	-8.12	-7.98
B_{1g}	π	-6.51	-6.40	-13.30	-12.10	-15.27	-14.18	1.01	1.06	-7.47	-7.42
B_{2g}	π	-5.30	-5.51	-13.28	-12.18	-14.90	-14.37	0.58	0.88	-6.34	-6.82
B_{3u}	π^*	-2.86	-2.97	-13.08	-11.86	-8.78	-8.17	-1.82	-0.90	-0.37	-0.19
A_u	π^*	-1.58	-1.59	-13.18	-11.62	-8.49	-7.92	-2.21	-1.38	0.89	0.74
B_{1g}	π^*	-1.25	-1.28	-12.89	-11.63	-7.63	-7.34	-2.54	-1.83	1.47	1.18
B_{3u}	π^*	-0.52	0.01	-11.90	-11.41	-6.47	-6.94	-2.84	-2.45	2.07	2.03

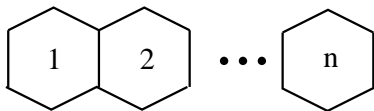


FIG. 2: Schematic viewgraph of the polyacenes: n is the number of monomers.

$n = 2$, anthracene $n = 3$, tetracene $n = 4$ and so on. These systems have received much attention because of their potential use in efficient organic thin film devices. Theoretically they have been characterized quite widely [50, 51, 52, 53, 54, 55, 56] and recently also an investigation in the context of the GW approximation appeared, where polymorphs of the pentacene crystal were analyzed in terms of their optical spectra [57].

Here, the polyacenes are chosen as a prototypical π -system to explore the accuracy of our approximations. To this end we fully optimized the different structures at the DFTB level of theory without imposing symmetry constraints. The obtained geometries are in excellent agreement with a recent DFT study on the polyacenes from $n = 1$ to 5, in which the hybrid functional B3LYP and the accurate 6-311G** basis set was employed [54]. For all the molecules studied, we find a mean deviation in the bond lengths of no more than 0.005 Å. Then the quasiparticle spectrum was obtained according to the approximations in the last section. For comparison, also first principles GW calculations in the Gaussian type orbital (GTO) implementation of Ref. [22] were carried out. In the ab-initio GW calculation, the wave functions have

been represented by s and p Gaussian orbitals on carbon (decay constants: 0.12, 0.4, 1.0, and 2.8 atomic units, i.e., 16 orbitals per atom) and by s and p orbitals on hydrogen (decay constants 0.15, 0.4 and 1.0, i.e., 12 orbitals per atom). The two-point functions occurring in the GW scheme are represented by s, p, d, and s* orbitals on carbon (decay constants 0.2, 0.6, 1.6, and 4.0, i.e., 40 orbitals per atom) and on hydrogen, as well (decay constants 0.25 and 0.7, i.e., 20 orbitals per atom). In both the DFTB and first principles calculations the LDA exchange-correlation functional was used.

The results for benzene and anthracene are listed in Tab. II for a small number of states around the frontier orbitals, according to the energy partitioning of Eq. (2). Focusing first on the orbital energies, we find a very good agreement between the DFTB and the first principles results. This might be surprising considering the limited basis set employed in the former approach. However, the DFTB basis consists of optimized atomic orbitals rather than simple Gaussian type orbitals. Moreover, the approximations underlying the DFTB method seem to be justified due to a stable error cancellation for the π -orbitals. This holds true to a lesser extent for σ -orbitals, like the E_{2g} state in benzene, where an error up to 0.6 eV is found. Not unexpected, difficulties are also observed for unbound virtual orbitals like the B_{2g} state in benzene, since the description of the continuum is very sensitive to the quality of a finite basis set.

Next, we turn to the exchange-correlation energy per orbital. Here we find in comparison with the first principles results, that the DFTB values are in general too positive by roughly 10 %. However, the error even reaches

20 % for the σ -orbitals of benzene. We attribute this failure to the neglect of crystal field terms in our approach, which is likely to have different effects on orbitals of σ and π symmetry. In fact, we calculated elements of the type $\langle \phi_\mu^A | v_{xc}(\rho_B) | \phi_\nu^A \rangle$ and found, that integrals where A represents a hydrogen atom and B a carbon atom are significantly larger than in the reversed situation or integrals where both A and B stand for carbon atoms. As the latter two types of integrals occur in the calculation of π -orbitals of the polyacenes, while the first one is important for σ -orbitals, the missing of the crystal field terms is likely to be the source of error here.

Considering now the exchange contribution to the self-energy Σ_x^i , similar trends are found. Compared to the ab initio results, the DFTB values are slightly too positive. Since the terms Σ_x^i and v_{xc}^i contribute in Eq. (2) with opposite signs to the quasiparticle energies, a stable error cancellation is expected. A larger deviation is found again for the E_{2g} state in benzene, where an error up to 4 eV occurs. Since the exchange integrals depend strongly on the atomic repulsion integrals U_{ee} in our approximation, the error could be reduced by enlarging this parameter for hydrogen without losing the good performance for the π -orbitals. However, we hesitate to treat the U_{ee} values as empirical parameters, because of loss of transferability. Instead, one should look for a better approximation of the two-electron integrals. In our approximation the density $\phi_\mu(\mathbf{r})\phi_\nu(\mathbf{r})$ is represented by a superposition of spherical charge densities. Consequently, the two-electron integrals are given by simple monopole-monopole interactions, thus neglecting any angular momentum dependence. A natural next step would be to include higher order terms in a multipole expansion of the density $\phi_\mu(\mathbf{r})\phi_\nu(\mathbf{r})$, as it is done in the semiempirical MNDO method developed by Dewar and Thiel [58].

Next, the final quasiparticle energies are discussed. For the π -orbitals the mean deviation of the DFTB results from the ab initio values is 0.4 eV, with errors decreasing when the system size is increased. As could be already expected from the forgoing discussion, the description of σ -orbitals is less satisfactory in the current state of approximations. For the E_{2g} orbital of benzene an error of 1.25 eV is observed. For the unoccupied levels however, a very nice agreement between first principles and DFTB results is evident. Clearly, this is a consequence of an error cancellation between all terms in Eq. (2), since e.g. the correlation contribution Σ_c^i is systematically underestimated in the DFTB scheme.

In this context it is interesting to investigate if a more advanced treatment of the Dyson equation (1) leads to better results. In fact, it has been found that the associated wavefunctions of orbitals which are bound at the DFT level of theory, but unbound at the QP level, differ considerably. This is in contrast to the assumptions made in the derivation of Eq. (2) from Eq. (1) and hence the full QP Hamiltonian needs to be diagonalized in these cases and self-consistency with respect to the energy dependence of Σ must be achieved. Following this approach

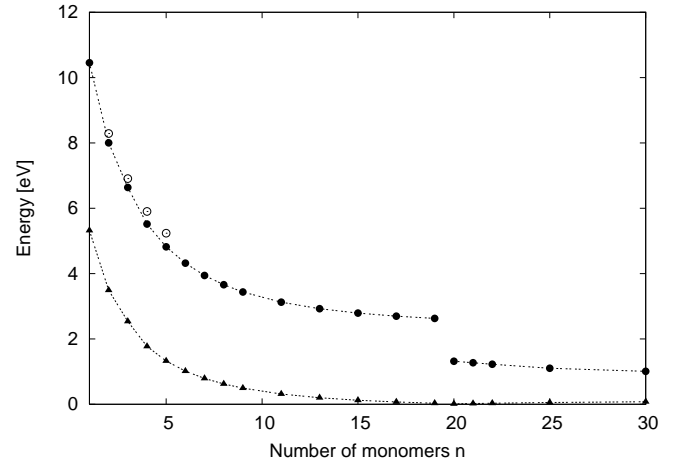


FIG. 3: Quasiparticle (\bullet) and DFT gap (\blacktriangle) for the lowest energy conformer of the polyacenes as obtained in the DFTB approximation. Lines are guides to the eyes. Shown is also the difference of experimentally determined electron affinities and vertical ionization potentials (\circ) from Ref. [60], where they were available.

earlier investigations of this point reported shifts of the LUMO level up to 0.8 eV [48, 59]. We also performed such calculations for benzene and found that even for the E_{2u} state the diagonalization changes the QP spectrum by less than 0.01 eV. This can be understood as a consequence of the minimal basis set we employ, which does not provide enough flexibility to describe the relaxation towards delocalized states. Considering the energy dependence of the self-energy, it can be stated that the approximate treatment of Eq. (2) using the renormalization constant Z is quite successful, as we find deviations less than 0.2 eV from the self-consistent solution of the Dyson equation.

B. Size dependence of the quasiparticle gap

After validation of the method, we now turn to a first application and analyze in the following the quasiparticle gap $\epsilon_{\text{gap}}^{QP} = \epsilon_{\text{LUMO}}^{QP} - \epsilon_{\text{HOMO}}^{QP}$ as a function of chain length. The first observation which can be drawn from Fig. 3 is that the DFTB quasiparticle gap is in very nice agreement with the experimental data, which provides some confidence that the general trends we are looking for are correctly described. Furthermore, Fig. 3 shows that the DFT gap is continuously decreasing and almost vanishes for $n = 19$ monomers. As the length increases, the geometry of the innermost part of the chain resembles more and more that of two coupled polyacetylene chains with equal bond lengths, as schematically depicted in Fig. 4. The vanishing of the DFT gap can thus be understood in terms of a simple particle-in-a-box model.

In stark contrast to the DFT gap, $\epsilon_{\text{gap}}^{QP}$ remains finite for increasing chain length and it seems worthwhile to

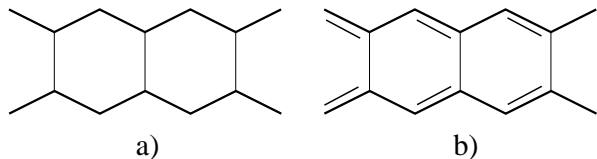


FIG. 4: Schematic representation of the lowest energy conformations of the polyacenes found in this study. The aromatic structure a) is the most stable for $n \leq 19$, while the Peierls (Z)-distorted structure b) is energetically favoured for $n \geq 20$.

explore the physical origin of this different behaviour in a short digression. In fact, QP energies can be directly compared to results from photoemission and inverse photoemission measurements, i.e., they include the effect of an extra particle, while DFT is a pure N-electron theory. Delerue et al. pointed out that for nanocrystals the size dependence of the difference $\Delta = \epsilon_{\text{gap}}^{\text{QP}} - \epsilon_{\text{gap}}^{\text{DFT}}$ can be estimated on the basis of classical electrostatic arguments [31]. Considering the interaction between the extra particle and its induced surface charge on the nanocrystal, they arrived at the following formula:

$$\Delta \approx \left(1 - \frac{1}{\epsilon(R)}\right) \frac{e^2}{R} + 0.94 \frac{e^2}{\epsilon(R)R} \left(\frac{\epsilon(R) - 1}{\epsilon(R) + 1}\right) + \Delta_b, \quad (24)$$

where $\epsilon(R)$ is an effective dielectric constant and Δ_b is the bulk value of Δ . In order to apply Eq. (18) to the polyacenes, we took R to be half of the chain length and obtained $\epsilon(R)$ by averaging the microscopic dielectric function in Eq. (19). The obtained values increase from 1.72 for $n = 1$ to 2.14 for $n = 19$, which reflects the decreasing band gap. A fit of Eq. 18 to our QP results is shown in Fig. 5 and leads to a value of 2.18 eV for Δ_b . Taking into account that the DFT gap is vanishing for $n \rightarrow \infty$, we therefore predict a QP gap of the same value for an infinite chain in the aromatic structure of Fig. 4. Inspection of Fig. 5 further reveals that for $n > 4$ the agreement between Delerue's formula and the QP results is excellent. The fact that Eq. (18), which was developed in the context of nanocrystals also holds for a quasi one-dimensional system like the polyacenes is quite remarkable.

We now continue the discussion of Fig. 3. Between $n = 19$ and $n = 20$ HOMO and LUMO cross, which has important implications for the geometrical as well as electronic structure of the system. Remaining in the picture of polyacene as coupled polyacetylene, we observe that the equal C-C bond lengths found for $n < 20$ turn into alternating single and double bonds for larger n as depicted in Fig. 4, i.e., the system undergoes a Peierls distortion. In contrast to polyacetylene, where the bond alternation is found to be around 0.08 \AA [61], the effect is much weaker here with a value of less than 0.008 \AA . Nevertheless, the dimerization leads like in polyacetylene to an opening of the DFT gap, which tends towards a small but finite value for the infinite chain. Inspection of Fig. 3 shows that also the quasiparticle gap differs significantly

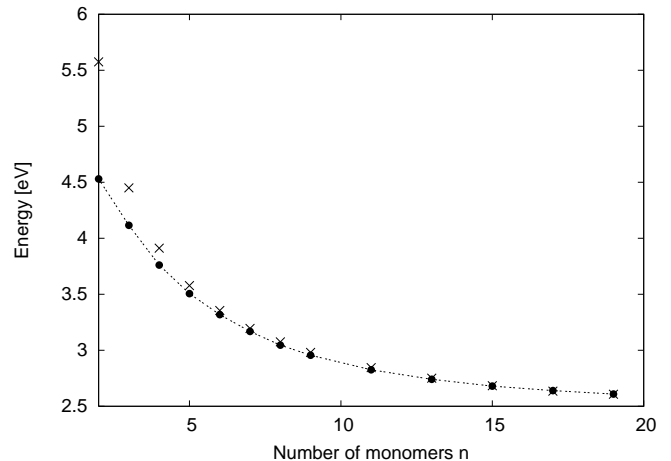


FIG. 5: Fit of Eq. (18) (x) to the difference between QP and DFT gap as obtained in this work (•).

for the distorted and undistorted structure. This fact could be used in experiment to discriminate between both polymorphs, since we find in line with the MP2 results of Cioslowski [52], that the two forms are energetically quite close and should therefore coexist in real samples. We should mention however, that up to now only polyacenes up to $n = 6$ could be isolated, since larger chains are highly vulnerable to photooxidation [55].

The results of this section can be summarized as follows. First, the aromatic form of the infinite polyacene is predicted to be metallic at the DFT level of theory, but semiconducting at the GW level. It thus provides another example besides bulk Ge [24], where the DFT gap is not only quantitatively but also qualitatively wrong. Second, the difference between the DFT and QP gap can be understood in terms of the interaction between an extra particle - which is missing in DFT - and the charge it induces on the molecular surface. Third, the Peierls distorted polyacene conformer is energetically favoured only for very long chains and possesses a QP spectrum which is markedly different from the aromatic form. This also underlines the usefulness of approximate GW schemes, since in a first principles context the Peierls transition found here might not be noticed due to the limited treatable system size [62].

IV. NUMERICAL CONSIDERATIONS

In the following, we shortly discuss the numerical efficiency of our approximations. The method scales like $N^2 N_l^2$, where N is the number of basis functions and N_l is the number of spherically averaged basisfunctions, that are used in the representation of two-point functions ($N_l < N$). This has to be compared to first principles implementations, which usually scale like N^4 . An additional reduction of computation time is obtained, since we use a minimal basis of optimized atomic orbitals,

while in a first principles framework a larger number of primitive orbitals is required. Moreover, the scaling prefactor is reduced in the DFTB scheme, because the necessary integrals are either precalculated and tabulated or approximated by simple functions. As an example, the first principles evaluation of the QP spectrum of anthracene took 170 minutes on a Pentium Xeon 2.20 GHz processor (including 120 minutes for the DFT part of the calculation), compared to less than 1 second on a Pentium 4 with 2.40 GHz in our approach. The largest structure we studied, the $n = 30$ polyacene with 186 atoms took 10 minutes. The limiting factor in the calculation of very large systems is therefore not the computation time but rather the memory requirement. We try to circumvent this problem by computing memory intensive quantities like the overlap charges q_{μ}^{ij} on-the-fly in a direct way.

V. CONCLUDING REMARKS

In this work we presented a method to perform quasiparticle calculations of molecular systems at a highly reduced computational cost compared to first principles im-

plementations. The scheme was applied to hydrocarbons, but it can be easily extended to other elements, since all required parameters are calculated from first principles. The various approximations of the method are intended to be as consistent as possible with the underlying DFTB approach to allow for a stable error cancellation. For benzene and anthracene the results are indeed comparable with higher level calculations with the exception of σ -orbitals. Here, ways to overcome the deficiencies were outlined. Nevertheless, we think that the scheme could be useful already at the present stage, since e.g. for optical spectra or in the electronic transport only a few states around the Fermi level are active and dominate the physical properties of a system.

Acknowledgements

The authors would like to thank Alessandro Pecchia and Alessio Gagliardi for fruitful discussions related to this work. Further, the EC-Diode-Network is gratefully acknowledged for financial support and T.A.N is much obliged for using the computer facilities at the German Cancer Research Center in Heidelberg.

-
- [1] F. Bechstedt, *Adv. Solid State Phys.* **32**, 161 (1992).
 - [2] C.-O. Almbladh and U. von Barth, *Phys. Rev. B* **31**, 3231 (1985).
 - [3] R. van Leeuwen and E. J. Baerends, *Phys. Rev. A* **49**, 2421 (1994).
 - [4] A. Görling, *Phys. Rev. A* **54**, 3912 (1996).
 - [5] L. Hedin, *Phys. Rev. A* **139**, 796 (1965).
 - [6] M. Rohlfing and S. G. Louie, *Phys. Rev. Lett.* **80**, 3320 (1998).
 - [7] M. Rohlfing, *Int. J. Quant. Chem.* **80**, 807 (2000).
 - [8] Y. Ohta, J. Maki, T. Yoshimoto, Y. Shigeta, H. Nagao, and K. Nishikawa, *Int. J. Quant. Chem.* **84**, 348 (2001).
 - [9] S. Ishii, K. Ohno, and Y. Kawazoe, *Mat. Trans.* **45**, 1411 (2004).
 - [10] P. Nozières, *Theory of Interacting Fermi Systems* (Benjamin, New York, 1964).
 - [11] L. J. Sham and T. M. Rice, *Phys. Rev.* **144**, 708 (1966).
 - [12] G. Strinati, *Phys. Rev. B* **29**, 5718 (1984).
 - [13] E. K. U. Gross and W. Kohn, *Adv. Quantum Chem.* **21**, 255 (1990).
 - [14] G. Onida, L. Reining, and A. Rubio, *Rev. Mod. Phys.* **74**, 601 (2002).
 - [15] A. Dreuw, J. L. Weisman, and M. Head-Gordon, *J. Chem. Phys.* **119**, 2943 (2003).
 - [16] M. Wanko, M. Garavelli, F. Bernardi, T. A. Niehaus, T. Frauenheim, and M. Elstner, *J. Chem. Phys.* **120**, 1674 (2004).
 - [17] Y. Tawada, T. Tsuneda, S. Yanagisawa, T. Yanai, and K. Hirao, *J. Chem. Phys.* **120**, 8425 (2004).
 - [18] O. Gritsenko and E. J. Baerends, *J. Chem. Phys.* **121**, 655 (2004).
 - [19] M. A. Reed, C. Zhou, C. J. Muller, T. P. Burgin, and J. M. Tour, *Science* **278**, 252 (1997).
 - [20] M. Di Ventura, S. T. Pantelides, and N. D. Lang, *Phys. Rev. Lett.* **84**, 979 (2000).
 - [21] A. Pecchia and A. Di Carlo, *Rep. Prog. Phys.* **67**, 1497 (2004).
 - [22] M. Rohlfing, P. Krüger, and J. Pollmann, *Phys. Rev. B* **52**, 1905 (1995).
 - [23] M. Rohlfing, P. Krüger, and J. Pollmann, *Phys. Rev. B* **54**, 13759 (1996).
 - [24] M. S. Hybertsen and S. G. Louie, *Phys. Rev. B* **34**, 5390 (1986).
 - [25] F. Bechstedt, R. Del Sole, G. Cappellini, and L. Reining, *Solid State Comm.* **84**, 765 (1992).
 - [26] M. Palumbo, R. Del Sole, L. Reining, F. Bechstedt, and G. Cappellini, *Solid State Comm.* **95**, 393 (1995).
 - [27] P. A. Sterne and J. C. Inkson, *J. Phys. C: Solid State Phys.* **17**, 1497 (1984).
 - [28] F. Bechstedt and R. Del Sole, *Phys. Rev. B* **38**, 7710 (1988).
 - [29] Z.-Q. Gu and W. Y. Ching, *Phys. Rev. B* **49**, 10958 (1994).
 - [30] C. Delerue, M. Lannoo, and G. Allan, *Phys. Rev. B* **56**, 15306 (1997).
 - [31] C. Delerue, M. Lannoo, and G. Allan, *Phys. Rev. Lett.* **84**, 2457 (2000).
 - [32] J. Furthmüller, G. Cappellini, H.-Ch. Weissker, and F. Bechstedt, *Phys. Rev. B* **66**, 045110 (2002).
 - [33] D. Porezag, Th. Frauenheim, Th. Köhler, G. Seifert, and R. Kaschner, *Phys. Rev. B* **51**, 12947 (1995).
 - [34] M. Elstner, D. Porezag, G. Jungnickel, J. Elsner, M. Haugk, Th. Frauenheim, S. Suhai, and G. Seifert, *Phys. Rev. B* **58**, 7260 (1998).
 - [35] Please note that in the original formulation of Ref. [34] the Mulliken charges were not resolved according to the

angular momentum. The higher flexibility offered by the formulation in this work has only marginal influence on ground state properties, but is crucial for the description of exchange integrals that are needed here.

- [36] F. Aryasetiawan and O. Gunnarsson, Rep. Prog. Phys. **61**, 237 (1998).
- [37] W. G. Aulbur, L. Jönsson, and J. W. Wilkins, Solid State Phys. **54**, 1 (1999).
- [38] B. Farid in *Electron Correlation in the Solid State* edited by N. H. March (World Scientific, Imperial College, 1999), p. 103.
- [39] L. Hedin, J. Phys. Cond. Mat. **11**, R489 (1999).
- [40] W.-D. Schöne and A. G. Eguiluz, Phys. Rev. Lett. **81**, 1662 (1998).
- [41] T. Frauenheim, G. Seifert, M. Elstner, T. Niehaus, C. Köhler, M. Amkreutz, M. Sternberg, Z. Hajnal, A. Di Carlo, and S. Suhai, J. Phys. Cond. Mat. **14**, 3015 (2002).
- [42] T. A. Niehaus, M. Elstner, Th. Frauenheim, and S. Suhai, THEOCHEM **541**, 185 (2001).
- [43] I. Guseinov, B. Mamedov, and A. Rzaeva, J. Mol. Mod. **8**, 145 (2002).
- [44] J. Ridley and M. C. Zerner, Theo. Chem. Acta **32**, 111 (1973).
- [45] $\langle \phi_\mu \phi_\nu | \phi_\mu \phi_\nu \rangle = \iint \frac{\phi_\mu(\mathbf{r}) \phi_\nu(\mathbf{r}) \phi_\mu(\mathbf{r}') \phi_\nu(\mathbf{r}')}{|\mathbf{r} - \mathbf{r}'|} d\mathbf{r} d\mathbf{r}'$.
- [46] W. von der Linden and P. Horsch, Phys. Rev. B **37**, 8351 (1988).
- [47] R. W. Godby and R. J. Needs, Phys. Rev. Lett. **62**, 1169 (1989).
- [48] S. Ishii, K. Ohno, Y. Kawazoe, and S. G. Louie, Phys. Rev. B **63**, 155104 (2001).
- [49] Traditionally, the U^H parameters are calculated from an uncompressed wavefunction in the DFTB approach. To be consistent, we obtain the U^{ee} parameters in the same way here, although this is somewhat inconsistent with the treatment of the exchange energy, where values from a compressed wavefunction are used.
- [50] M.-H. Whangbo, R. Hoffmann, and R. B. Woodward, Proc. Roy. Soc. London A **366**, 23 (1979).
- [51] N. Trinajstić, T. G. Schmalz, T. P. Živković, S. Nikolić, G. E. Hite, D. J. Klein, and W. A. Seitz, New J. Chem. **15**, 27 (1991).
- [52] J. Cioslowski, J. Chem. Phys. **98**, 473 (1993).
- [53] M. K. Sabra, Phys. Rev. B **53**, 1269 (1996).
- [54] K. Wiberg, J. Org. Chem. **62**, 5720 (1997).
- [55] R. Notario and J.-L. M. Abboud, J. Phys. Chem. A **102**, 5209 (1998).
- [56] M. S. Deleuze, L. Claes, E. S. Kryachko, and J.-P. Francois, J. Chem. Phys. **119**, 3106 (2003).
- [57] M. L. Tiago, J. E. Northrup, and S. G. Louie, Phys. Rev. B **67**, 115212 (2003).
- [58] M. J. S. Dewar and W. Thiel, J. Am. Chem. Soc. **99**, 4899 (1977).
- [59] M. Rohlfing and S. G. Louie, Phys. Rev. B **62**, 4927 (2000).
- [60] *Ion Energetics Data* in *NIST Chemistry Webbook*, *NIST Standard Reference Database* Number 69, edited by P.J. Linstrom and W.G. Mallard (National Institute of Standards and Technology, Gaithersburg, MD, 2001) (<http://webbook.nist.gov>).
- [61] S. Suhai, Phys. Rev. B **27**, 3506 (1983).
- [62] The TDDFT study of Houk *et. al.* [63] investigated chains up to $n = 15$ and found no signature of Peierls distortion.
- [63] K. N. Houk, P. S. Lee, and M. Nendel, J. Org. Chem. **66**, 5517 (2001).